

Role of guanylate binding protein-1 in vascular defects associated with chronic inflammatory diseases

Matthias Hammon^a, Martin Herrmann^b, Oliver Bleiziffer^a, Galyna Pryymachuk^a, Laura Andreoli^c, Luis E. Munoz^b, Kerstin U. Amann^d, Michele Mondini^e, Marisa Gariglio^e, Paolo Airó^c, Vera S. Schellerer^f, Antonis K. Hatzopoulos^g, Raymund E. Horch^a, Ulrich Kneser^a, Michael Stürzl^h, Elisabeth Naschberger^{h*}

^a Department of Plastic and Hand Surgery, University Medical Center Erlangen, Erlangen, Germany

^b Institute for Clinical Immunology and Rheumatology, Department for Internal Medicine 3, University Medical Center Erlangen, Erlangen, Germany

^c Rheumatology and Clinical Immunology, University Clinic of Brescia, Piazzale Spedali Civili, Brescia, Italy

^d Division of Nephropathology, Institute of Pathology, University Medical Center Erlangen, Erlangen, Germany

^e Department of Clinical and Experimental Medicine, University of Piemonte Orientale, Novara, Italy

^f Department of Surgery, University Medical Center Erlangen, Erlangen, Germany

^g Division of Cardiovascular Medicine, Department of Medicine, Vanderbilt University School of Medicine, Nashville, TN, USA

^h Division of Molecular and Experimental Surgery, Department of Surgery, University Medical Center Erlangen, Erlangen, Germany

Received: February 9, 2010; Accepted: June 25, 2010

Abstract

Rheumatic autoimmune disorders are characterized by a sustained pro-inflammatory microenvironment associated with impaired function of endothelial progenitor cells (EPC) and concomitant vascular defects. Guanylate binding protein-1 (GBP-1) is a marker and intracellular regulator of the inhibition of proliferation, migration and invasion of endothelial cells induced by several pro-inflammatory cytokines. In addition, GBP-1 is actively secreted by endothelial cells. In this study, significantly increased levels of GBP-1 were detected in the sera of patients with chronic inflammatory disorders. Accordingly we investigated the function of GBP-1 in EPC. Interestingly, stable expression of GBP-1 in T17b EPC induced premature differentiation of these cells, as indicated by a robust up-regulation of both Flk-1 and von Willebrand factor expression. In addition, GBP-1 inhibited the proliferation and migration of EPC *in vitro*. We confirmed that GBP-1 inhibited vessel-directed migration of EPC at the tissue level using the rat arterio-venous loop model as a novel quantitative *in vivo* migration assay. Overall, our findings indicate that GBP-1 contributes to vascular dysfunction in chronic inflammatory diseases by inhibiting EPC angiogenic activity *via* the induction of premature EPC differentiation.

Keywords: rheumatic autoimmune disorders • guanylate binding protein-1 • endothelial progenitor cells • inflammation • systemic lupus erythematosus • rheumatoid arthritis • systemic sclerosis

Introduction

Blood vessel formation in adults may proceed through various pathways. The primary mechanism is angiogenesis by either sprouting or intussusception, both being vascular endothelial

growth factor (VEGF)-dependent processes [1, 2]. In addition, a VEGF-independent mechanical or looping angiogenesis has been described [3]. Vasculogenesis, previously regarded to be exclusively involved in vessel formation in the embryo, has also been shown to contribute to vessel formation in adults. This process involves the recruitment of endothelial progenitor cells (EPC) released from the bone marrow and incorporated into growing vessels in adults [1, 4]. The molecular characteristics and the isolation of these cells are still a matter of debate [5].

The most commonly used EPC markers are CD34, vascular endothelial cell growth factor receptor 2 (VEGF-R2/Flk-1), Tie2,

*Correspondence to: Dr. Elisabeth NASCHBERGER, Division of Molecular and Experimental Surgery, Department of Surgery, University Medical Center Erlangen, Schwabachanlage 10, 91054 Erlangen, Germany. Tel.: +49-9131-85-39141 Fax: +49-9131-85-32077 E-mail: elisabeth.naschberger@uk-erlangen.de

stem cell antigen-1 and CD133 (AC133). However, none of these molecules is specific for EPC [5, 6]. Because of their low abundance (0.01 to 0.0001%), the isolation of EPC is technically difficult [5]. In addition, mature endothelial cells, probably released from vessel walls, circulate in the peripheral blood and share common markers with the EPC [5, 6]. A large body of evidence indicates that EPC contribute to the formation of new vessels upon vascular injury, chronic inflammatory, hypoxic conditions and tumour growth [7–10].

In the rheumatic autoimmune disorders rheumatoid arthritis (RA), systemic lupus erythematosus (SLE) and systemic sclerosis (SSc), reduced numbers of circulating EPC have been described [11–14]. In RA, these cells display impaired migratory capabilities [13], possibly contributing to endothelial dysfunction associated with the increased cardiovascular morbidity and mortality commonly observed in these patients [15]. The molecular mechanism of EPC dysfunction is elusive. It has been suggested that chronic inflammation and increased levels of the pro-inflammatory cytokines interferon (IFN)- α/γ , tumour necrosis factor (TNF)- α or interleukin (IL)-1 α/β [16–18] may be involved in this process. This was partly confirmed by the finding that anti-TNF- α treatment restored EPC levels in RA patients [19].

Guanylate binding protein-1 (GBP-1) is a member of the family of large GTPases, which includes antiviral Mx proteins and the caveolae regulatory molecule dynamin [20–24]. GBP-1 expression is induced in endothelial cells by IFN- γ/α , IL-1 β/α and TNF- α [25] and mediates the potent anti-angiogenic effects of these cytokines, both *in vitro* and *in vivo* [26–28]. It inhibits endothelial cell proliferation, migration and invasiveness *in vitro* [26–28]. The anti-angiogenic effect of GBP-1 has recently been confirmed in colorectal carcinoma patients, where it was associated with sustained reduction of intratumoral angiogenic activity and improved cancer-related survival [29]. Interestingly, GBP-1 was described as the first GTPase secreted from endothelial cells. Secretion occurs *via* non-classical secretion pathways and was confirmed *in vivo* by the detection of increased GBP-1 concentrations in the cerebrospinal fluid of patients with bacterial meningitis [30].

Here we show that the levels of GBP-1 are increased in sera of patients with the rheumatic autoimmune diseases RA, SLE and SSc, which are characterized by chronic inflammatory vessel activation. We provide experimental evidence that GBP-1 is directly involved in the endothelial dysfunction and the regulation of EPC activity.

Materials and methods

Patient characteristics

Patients with SLE from the outpatient clinic of the Department of Internal Medicine 3 of the Erlangen University Medical Center met the diagnostic criteria of the American College of Rheumatology [31]. Patients with RA were from the Division of Rheumatology of the University of Heidelberg

that met the diagnostic criteria of the American College of Rheumatology [32]. Control samples were obtained from normal healthy volunteers. The study was approved by the Institutional Review Boards of the University of Erlangen – Nuremberg and Heidelberg. Written informed consent was obtained from all individuals before entering the study.

SSc patients were from Spedali Civili di Brescia. All patients fulfilled the criteria for SSc proposed by the American College of Rheumatology according to the classification system proposed by LeRoy *et al.* [33]. Thirty-two patients (34.8%) had a diffuse cutaneous SSc, whereas 60 (65.2%) were affected by the limited cutaneous form of the disease. Written consent was obtained by all of the patients included. A summary of the main patient characteristics is presented in Table 1.

Cell culture and stable transfection

T17b murine embryonic EPC [34, 35] were cultured in DMEM (Invitrogen, Carlsbad, CA, USA) with 20% foetal calf serum (Biochrom, Berlin, Germany), 100 U/ml penicillin, 100 μ g/ml streptomycin, 0.1 mM β -mercaptoethanol, 1 mM non-essential amino acids and 2 mM 4-(2-hydroxyethyl)-1-piperazineethanesulfonic acid (HEPES) buffer pH 7.5 (all purchased from Invitrogen) at 37°C in a humidified atmosphere at 5% CO₂. EPC were maintained in T-75 culture flasks (Nunc, Wiesbaden, Germany) coated for at least 2 hrs with 0.1% bovine skin gelatine, type B (Sigma-Aldrich, Taufkirchen, Germany) in phosphate-buffered saline (PBS) (Biochrom AG, Berlin, Germany). The cells were subcultured using 1 \times 0.5 g/l trypsin and 0.2 g/l ethylenediaminetetraacetic acid in HBSS (trypsin/EDTA) (PAA, Pasching, Austria) and passaged in a 1:8 ratio. Cells were counted using the CASY cell counting system (Schärfe System, Model DT, Reutlingen, Germany). All cells were regularly tested for mycoplasma infection by using MycoAlert (Cambrex, Charles City, IA, USA); all results were negative.

EPC were seeded in pre-coated 6-well plates with a density of 1 \times 10⁵ cells/well and cultured for 24 hrs. EPC were transfected with 2 μ g plasmid DNA using Effectene transfection reagent (Qiagen, Hilden, Germany) according to the manufacturer's instructions. The plasmids pMCV-2.2 (vector obtained from Mologen GmbH, Berlin, Germany) and pMCV-2.2-Flag-GBP-1 were used [30]. All plasmids contained a G418-resistance gene. Selection was performed with 500 μ g/ml G418 (PAA) for 10 days. Control-EPC were pooled after selection. For GBP-1-EPC, single clones were picked, subcultured and analysed for expression. Protein extracts of confluent T-25 were stored at –20°C until analysis.

Proliferation assay

Control- and GBP-1-EPC (4 \times 10³ cells) were seeded in 24-well plates, and three wells per group were counted using the CASY cell counting system (Schärfe System) after 3 hrs (day 0) for normalization. Every day until day 3 three wells of each group were counted. Proliferation is expressed as fold induction, and all experiments were performed in triplicates. One representative experiment of at least three is shown.

Wound-healing assay

The wound-healing assay was performed as described previously [28]. Briefly, control- and GBP-1-EPC were grown on gelatine-coated 6-well plates (Nunc) until confluence. Confluent cell monolayers of control- and GBP-1-EPC were scratched using a sterile 1 ml pipette tip. The monolayers were

Table 1. Clinical and demographic characteristics of the NHD (*n* = 80), RA (*n* = 50), SLE (*n* = 51) and SSc patients (*n* = 92) analysed

NHD (<i>n</i> = 80)		
Age (mean ± S.D.)*	31.8 ± 11.6 years	
Sex (females)†	43 (53.75%)	
RA (<i>n</i> = 50)		
Age (mean ± S.D.)	56.4 ± 13.3 years	
Females	37 (74%)	
At least four criteria of the following seven criteria were fulfilled for each patient:		
Morning stiffness ≥ 1 hr		
Arthritis of three or more joints (right/left PIP, MCP, wrist, elbow, knee, ankle and MTP joints)		
Arthritis of wrist, MCP or PIP joint		
Symmetric involvement of joints		
RA-typical radiographic changes in the hands		
Subcutaneous nodules		
Positive serum rheumatoid factor		
Activity parameter:		
Disease activity score (28 joints)‡	Remission < 2.6	19 (38%)
	Low activity < 3.2	12 (24%)
	Moderate activity 3.2–5.1	12 (24%)
	High activity > 5.1	3 (6%)
Erythrocyte sedimentation rate (ESR; mean ± S.D.)#	19.7 ± 18.2 mm/hr	
C-reactive protein (mg/l)§	≤2 mg/l	15 (30%)
	2–10.0 mg/l	26 (52%)
	10.1–40 mg/l	6 (12%)
	>40 mg/l	1 (2%)
SLE (<i>n</i> = 51)		
Age (mean ± S.D.)	40.2 ± 12.8 years	
Females	44 (86.3%)	
ESR (mean ± S.D.)#	28.0 ± 21.9 mm/hr	
C-reactive protein (mg/l)§	≤2 mg/l	24 (47.1%)
	2–10.0 mg/l	16 (31.4%)
	10.1–40 mg/l	7 (13.7%)
	>40 mg/l	2 (3.9%)
Leukocytes (mean ± S.D.)	6.5 ± 3.5 × 10 ³ /μl (normal: 4–10 × 10 ³ /μl)	
Lymphocytes (mean ± S.D.)	1.0 ± 0.8 × 10 ³ /μl (normal: 1.3–3.3 × 10 ³ /μl)	
Thrombocytes (mean ± S.D.)	241.0 ± 111.8 × 10 ³ /μl (normal: 140–400 × 10 ³ /μl)	
Positive serum rheumatoid factor§	11 (21.5%)	

Continued

Table 1. Continued

Autoantibody profile:	Anti-dsDNA antibodies (Farr; U/ml)	≤7.0: 23 (45.1%); >7.0: 28 (54.9%)
	Positive ANA titres	35 (68.6%)
	Anti-cardiolipin (GPL U/ml)**	≤13: 22 (43.1%); >13: 10 (19.6%)
	Positive lupus anticoagulant††	14 (27.5%)
	Anti-β ₂ -glycoprotein-1 (U/ml)‡‡	≤10: 19 (41.2%); >10: 4 (7.8%)
Organ involvement		
Joints	27 (52.9%)	
Kidneys	22 (43.1%)	
Skin	29 (56.9%)	
Blood	21 (41.2%)	
Vessels	5 (9.8%)	
Serous membranes	13 (25.5%)	
CNS	7 (13.7%)	
SSc (<i>n</i> = 92)		
Age (mean ± S.D.)	59.2 ± 13.1 years	
Females	82 (89%)	
Disease duration	10.8 ± 7.8 years	
Cutaneous form	Diffuse: 32 (35%)	Limited: 60 (65%)
Autoantibody profile:	Positive anti-nuclear antibodies	90 (97.8%)
	Anti-topoisomerase I (anti-Scl70)	26 (28.3%)
	Anti-centromere	30 (32.6%)
	Anti-RNA polymerase III	8 (8.7%)
Pulmonary fibrosis on CT scan	38 (41.3%)	
Restrictive lung disease (FVC, forced vital capacity <75%)	6 (6.5%)	
Left ventricular ejection fraction <55%	5 (5.4%)	
Diastolic left ventricular dysfunction based on E/A ratio	6 (6.5%)	
History of renal crisis	4 (4.3%)	
Prostacyclin endovenous therapy required for digital ulcerations	32 (34.8%)	

*Age of 10 donors was not registered.

†Sex of one donor was not registered.

‡DAS28 of four patients was not registered.

#ESR was not measured in five RA and two SLE patients.

§CRP was not measured in two RA and two SLE patients.

§Rheumatoid factor was not measured in 20 patients.

**Anti-cardiolipin was not measured in 19 patients.

††Lupus anticoagulant was not measured in 25 patients.

‡‡Anti-β₂-glycoprotein was not measured in 28 patients.

RA: rheumatoid arthritis; MCP: metacarpophalangeal; MTP: metatarsophalangeal; NHD: normal healthy donors; PIP: proximal interphalangeal; SLE: systemic lupus erythematosus; SSc: systemic sclerosis.

washed twice with PBS and cultured for 10 hrs in basal medium. Images of the same areas were taken immediately after scratching (0 hr) and every 2 hrs using an Olympus digital camera mounted on an Axiovert 25 microscope (Zeiss, Jena, Germany). The width of the wounding scratches at different time-points was measured and expressed as relative percentage of the initial distance at 0 hr, which was set to 100%. All experiments were performed in triplicates, and one representative experiment of at least three is shown.

Lactate dehydrogenase assay

Cell culture supernatants were taken of nearly confluent cells after 24 hrs. The cell number was determined at the time of harvesting. The lactate dehydrogenase activity assay was performed according to the manufacturer's instructions (CytoTox 96 non-radioactive cytotoxicity assay, Promega, Mannheim, Germany). The activity was normalized per 10^5 cells.

RNA isolation and RT-PCR

RNA isolation and RT-PCR was performed as previously described [24]. Briefly, total RNA of control- and GBP-1-EPC was isolated using the RNeasy Mini Kit (Qiagen) according to the manufacturer's instructions. Residual traces of genomic DNA were removed by DNase I (Qiagen) digestion. RNA concentration and purity were determined photometrically (GeneQuant, Amersham Biosciences, Freiburg, Germany), and RNA integrity was controlled by non-denaturing agarose gel electrophoresis. One microgram of total RNA from each sample underwent RT-PCR after DNase treatment. Reverse transcription and cDNA synthesis was done using SuperScript III Reverse Transcriptase (Invitrogen) followed by RT-PCR analysis using $10\times$ PCR buffer, 50 mM $MgCl_2$, Platinum *Taq* DNA polymerase and dNTPs (25 mM each) according to the supplemented protocols. The following primer pairs were used for the amplification of murine reverse-transcribed products: von Willebrand factor (vWF): forward 5'-GTGAAGATTGGCTGCAACAC-3'; reverse 5'-TGTGCTTCAGGACACAGAG-3'; flk (VEGFR-2): forward 5'-ATTCAGGCATTGACTGAGAG-3'; reverse 5'-TCCAAGTTGGTCTTTTCCCTG-3'; glyceraldehyde-3-phosphate dehydrogenase (mGAPDH): forward 5'-GCCTCGTCCCGTAGA-3'; reverse 5'-GATGCATTGCTGACAATCTTG-3'. The following primer pair was used for the amplification of human GBP-1: forward 5'-TCAGCTGACTTTGTGAGCTT-3'; reverse 5'-TCAGCCTGTATCCCCTTCT-3'. The murine flk (VEGFR-2) and GAPDH primer pairs have been published previously [36]. All reagents were purchased from Invitrogen. Ten microlitres of each PCR sample were electrophoresed on a 1% agarose gel containing ethidium bromide. RT-PCR products were photographed under a UV transilluminator and quantified using AIDA software (raytest, Straubenharth, Germany).

Western blot

Western blotting of Ripa cell lysates was performed as described previously [25, 30]. The following primary antibodies were incubated for 1 hr at room temperature (RT): monoclonal rabbit anti-murine actin antibody (1:1000; Sigma-Aldrich) and monoclonal rat anti-human GBP-1 antibody (clone 1B1; 1:500; hybridoma supernatant). Detection of the primary antibodies was performed with donkey anti-rabbit (GE Healthcare, Munich, Germany) and rabbit anti-rat (Dako, Hamburg, Germany) immunoglobulin G (IgG) coupled to horseradish peroxidase (HRP) (1:5000) for 45 min. at RT. HRP detection was performed with enhanced chemiluminescence (ECL) reagents (GE Healthcare) and x-ray films (Fuji, Düsseldorf, Germany).

Immunocytochemistry

Immunocytochemistry was performed as previously described [37]. Briefly, for all stainings the cells were cultured on gelatine-coated culture slides (BD Biosciences, Heidelberg, Germany) until they reached confluence. All slides were washed with PBS once and fixed in ice-cold ethanol for at least 20 min. Cells were rehydrated and blocked with 10% goat normal serum (GNS) (Dianova, Hamburg, Germany) in TBS. Afterwards, incubation with a monoclonal rat anti-human GBP-1 antibody (clone 1B1; hybridoma supernatant; 1:100 in 5% GNS in TBS) was done for 2.5 hrs. Subsequently, goat anti-rat immunoglobulin (Alexa 488; Invitrogen, Karlsruhe, Germany 1:500 in 5% GNS in TBS) was added for 1 hr. Nuclei were counterstained with 4',6-diamidin-2'-phenylindol-dihydrochloride (DAPI) (Invitrogen; 1:5000 in A.d.) for 20 min. Slides were mounted with fluorescence mounting medium (Dako) and photographed using an Aristoplan microscope (Leica Microsystems, Bensheim, Germany).

Differentiation of control- and GBP-1-EPC

Differentiation of EPC was induced by the application of differentiation medium (DM) containing retinoic acid and cyclic adenosine monophosphate (cAMP) on four consecutive days following a previously described protocol [34]. In brief, the DM was generated by supplementing normal medium with 0.5 mM dibutyryl cAMP (Sigma-Aldrich Chemie, Schnelldorf, Germany) and 1 μ M retinoic acid (Sigma Aldrich Chemie). Control- and GBP-1-EPC (1×10^6 cells) were seeded in pre-coated T-75 cell culture flasks (Nunc), and DM was added 5 hrs later. EPC were cultured with DM for 4 days. DM was refreshed each day. On day 5 the EPC were detached, counted using the automatic CASY cell counting system (Schärfe System) and lysed for RNA extraction. Lysates were stored at -80°C until analysis. Supernatants of the last 24 hrs were taken and stored at -80°C until analysis. As a control, 3.5×10^5 control- and GBP-1-EPC were cultured in pre-coated T-75 cell culture flasks (Nunc) with normal culture medium until they reached confluence. The non-differentiated cells were treated identically to the differentiated cells except for the lack of DM.

GBP-1-ELISA

Cell culture supernatants were taken of nearly confluent cell layers after 24 hrs and analysed in triplicates by GBP-1-ELISA according to a previously described protocol [30]. The cell number was determined at the time of harvesting. Serum samples were analysed in triplicates using the same protocol except with diluting the samples 1:8 before analysis. The colour reaction was measured in a microplate reader (Model 680; Bio-Rad, Munich, Germany). The results shown are depicted as means \pm S.D. and are normalized to the corresponding cell number for the cell culture supernatants.

Labelling of EPC

EPC were labelled using the Cell Tracker CM-Dil (Molecular Probes, Leiden, Netherlands). Accordingly, 1 mg Dil was dissolved in 1 ml dimethyl sulfoxide (DMSO), and 25 μ l of this stock were diluted in 10 ml of normal culture medium. Cells of a T-75 flask were incubated with the Dil-medium solution and kept at 37°C for 5 min., followed by 4°C for 15 min. After this procedure, the cells were detached, counted with the CASY cell counting system, and used for the experiments.

Arterio-venous loop (AV-loop) in the rat model system – experimental design and animals

Chambers containing 5×10^6 control- or GBP-1-EPC suspended in 500 μ l fibrin gel were implanted ($n = 8$). The explantation was performed 14 days after the implantation of the constructs. Syngenic male Lewis rats (Charles River Laboratories, Sulzfeld, Germany) with a mean weight of 250 ± 50 g were used in this study. The German regulations for the care and use of laboratory animals were followed at all times. All experiments were approved by the animal care committee of the University of Erlangen and the Government of Mittelfranken, Germany. The animals were housed in the veterinary care facility of the University Medical Center Erlangen and submitted to a 12 hr dark/light cycle with *ad libitum* access to standard chow (Altromin, Hamburg, Germany) and water.

Isolation chamber and composition of the fibrin matrix

The cylindrical chamber (inner diameter 10 mm, height 6 mm) with a rounded lid was made of heat-resistant medical-grade teflon (P. Greil, Department of Materials Science, Glass and Ceramics, University of Erlangen). In this study, the matrix was composed of a clinically approved fibrin gel (Tissucol, Baxter, Unterschleissheim, Germany) with a fibrinogen concentration of 10 mg/ml, a thrombin concentration of 2 IU/ml and an aprotinin concentration of 1500 KIE/ml to delay fibrinolysis.

Generation of the AV-loop

Operations were performed as previously described [38–40]. Briefly, all operations were performed by the same microsurgeon using an operative microscope (Zeiss) on rats under general anaesthesia with isoflurane (Baxter). The left femoral vessels were exposed by a longitudinal skin incision from the groin to the knee. The artery and vein were dissected from the pelvic artery in the groin to the bifurcation of the femoral artery in the knee. A 20 mm vein graft was harvested from the right femoral vessels. This vein graft was interposed between the recipient left femoral vein and artery by microsurgical techniques using 11–0 sutures (Ethicon, Norderstedt, Germany). The chamber was filled with 250 μ l fibrin gel, and the AV loop was passed around the four plastic sticks. Then, the chamber was filled with the second half of the fibrin gel-matrix to a total volume of 500 μ l, the lid was closed and the chamber was fixed in the groin using Prolene 3–0 (Ethicon) sutures. Haemostasis was assured, and the wound was closed using Vicryl 3–0 (Ethicon). Post-operatively, all animals received 0.4 ml long-term penicillin dihydrostreptomycin (aniMedica GmbH, Senden-Bösensell, Germany), buprenorphin (0.3 mg/kg body weight, Temgesic, Essex Chemie AG, Luzern, Switzerland) and heparine (80 IU/kg Liquemin, Ratiopharm, Germany).

Histological analysis

The animals were perfused with Microfil prior to explantation of the constructs. The abdomen was opened *via* a midline incision, and the aorta and inferior vena cava were exposed. After cannulation of the distal descending aorta using a 24-gauge catheter, the rats were flushed with 100 ml heparin solution in Ringer buffer (100 I.E./ml) until the returning fluid from the sev-

ered inf. vena cava was clear. Then, 20 ml yellow Microfil (MV-122) containing 5% MV Curing Agent (both Flowtech, Carver, MA, USA) were injected. Finally, the aorta and caval vein were ligated, and the rats were cooled at 4°C for 24 hrs.

The constructs were fixed in 4% formalin solution for 12 hrs, dehydrated in graded ethanol and embedded in paraffin. Cross-sections (3 μ m) were obtained using a Leica microtome (Leica Microsystems) after the constructs were cut in the middle. Planes were oriented rectangular to the longitudinal axis of the AV loop. Cross-sections were stained either using haematoxylin/eosin or DAPI (Invitrogen).

The images were evaluated by two independent and blinded observers. All images were generated with a Leica microscope and digital camera. Scale bars are given in the respective figures.

Statistical analysis

The Mann-Whitney *U*-test and Student's *t*-test for independent samples were performed with SPSS 15.0 software (SPSS Inc., Chicago, IL, USA). Level of significance was defined at $P < 0.05$.

Results

Sera levels of GBP-1 are increased in patients with systemic autoimmune diseases

Sera were drawn from patients suffering from RA, SLE or SSc, which are autoimmune diseases displaying severe inflammation and are known for having endothelial dysfunction. The main patient characteristics for all of the cohorts are summarized in Table 1. GBP-1 serum levels were quantified by ELISA and compared to sera of normal healthy donors (NHD). GBP-1 levels were significantly increased in all patient cohorts compared to the control group (Fig. 1, asterisks given for $P < 0.05$). The GBP-1 serum levels for RA, SLE, SSc and NHD were 190.6 ± 301.6 ng/ml (RA, $n = 50$, $P < 0.001$), 75.2 ± 188.0 ng/ml (SLE, $n = 51$, $P = 0.036$), 87.5 ± 295.2 ng/ml (SSc, $n = 92$, $P = 0.027$) and 17.5 ± 43.9 ng/ml (NHD, $n = 80$), respectively. The relative numbers of samples with GBP-1 concentrations higher than two standard deviations above the mean of the control group (Fig. 1, dashed line) were at least six times increased in the cohorts of autoimmune patients (RA: 40.0%, SLE, 17.6%; SSc, 15.2%; NHD 2.5%).

GBP-1 induces premature differentiation of EPC

GBP-1 expression in tissues is closely associated with endothelial cells [25]. In this framework it was interesting that impaired functions of circulating EPC have been described in patients with rheumatic autoimmune disorders [11–14]. Therefore, we aimed to investigate the function of GBP-1 in EPC. GBP-1 cDNA was stably expressed in the murine endothelial embryonic progenitor cell line T17b in order to investigate the role of GBP-1 in a well-defined

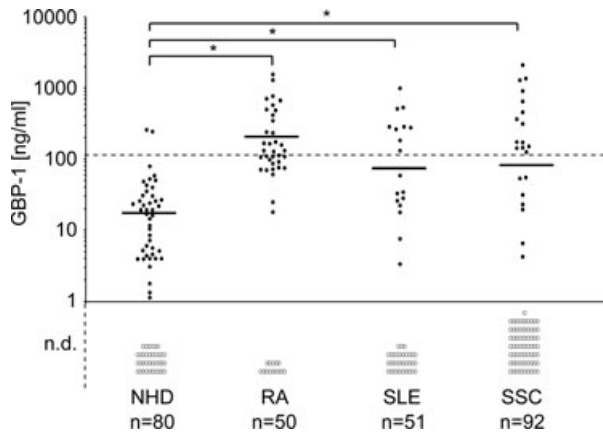


Fig. 1 GBP-1 levels are increased in sera of patients with the autoimmune diseases, rheumatoid arthritis (RA), systemic lupus erythematosus (SLE) or systemic sclerosis (SSc). GBP-1 was quantified by ELISA [30] in serum samples of patients suffering from RA ($n = 50$), SLE ($n = 51$), SSc ($n = 92$) and NHD ($n = 80$). A vertical scatter plot is given with a line corresponding to the mean values. A dashed line indicates the mean of the NHD plus two standard deviations. A t-test for independent samples was used to determine significance (asterisks given for P -values < 0.05). Non-detectable (n.d.) indicates GBP-1 values below the detection limit of the ELISA.

experimental model for EPC. Three cell clones, which exhibited GBP-1 expression levels similar to those observed in IFN- γ -treated human endothelial cells [26–28] (Fig. 2A, GBP-1) were selected and pooled for further studies. The cell population obtained showed a purity of more than 95% when GBP-1 expression was analysed at the single cell level by immunocytochemistry (Fig. 2B, GBP-1 pool). The control cells (control-EPC) stably transfected with the empty vector did not show any signal in analyses by Western blotting (Fig. 2A) or immunocytochemistry (Fig. 2B). Culture supernatants showed significantly elevated GBP-1 concentrations in GBP-1-transfected cells by ELISA (Fig. 2C, left). Cell lysis was not increased under these conditions, as shown by the quantification of lactate dehydrogenase in the same supernatants (Fig. 2C, right). The amount of GBP-1 present in the supernatant of GBP-1-EPC was similar to the amount previously described to be actively secreted from IFN- γ -stimulated HUVEC within the same period of time [30]. These results indicated that EPC similarly as differentiated endothelial cells secrete GBP-1, which may contribute to increased serum concentrations of this protein in patients with rheumatic autoimmune disorders.

Differentiation of T17b cells can be induced by treatment with cAMP and retinoic acid [34]. Analysis by immunocytochemistry showed that the induction of differentiation did not affect GBP-1 expression levels in these cells (Fig. 3A, compare differentiated [diff.] and undifferentiated [undiff.] cells). However, differentiated cells were enlarged and cell numbers were reduced, irrespective of GBP-1 expression (Fig. 3A). The same phenotypical changes (enlargement and reduced number of cells) were observed in differentiated control cells in the absence of GBP-1 expression (data not shown).

It has been shown that differentiation of T17b cells increases the expression of vascular endothelial growth factor receptor 2

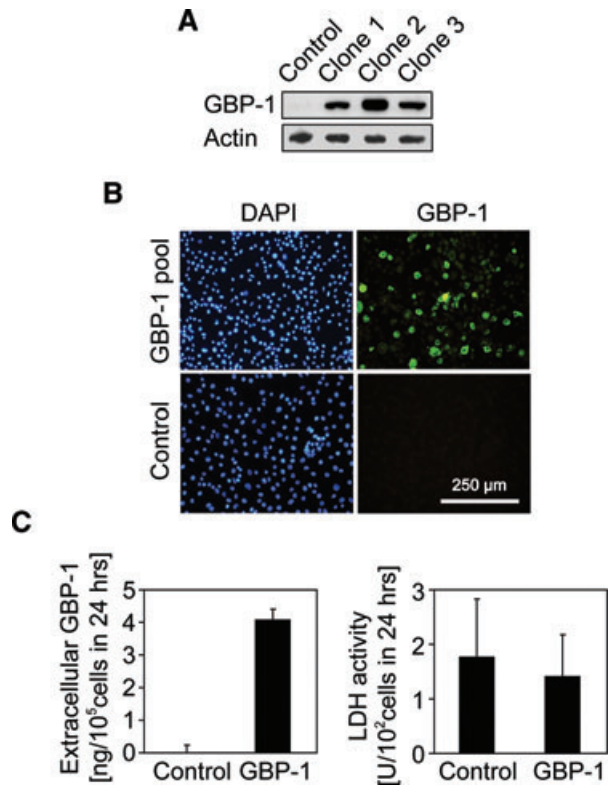


Fig. 2 Detection of GBP-1 expression and secretion in stably transfected EPC. (A) Western blot analysis of total cell lysates obtained from EPC clones stably transfected with control-vector pMCV-2.2 (control-EPC) or with flag-tagged GBP-1 (GBP-clones 1, 2 and 3). Immunochemical detection of actin demonstrates equal protein loading. (B) Control- and GBP-1-EPC were stained by immunocytochemistry for GBP-1 using a monoclonal rat anti-human GBP-1 antibody (clone 1B1) and an Alexa488-labelled secondary antibody. GBP-1-staining is visualized by green colour. Counterstaining was performed with DAPI (blue). (C) Extracellular GBP-1 was quantified in the culture supernatants of control- and GBP-1-EPC by ELISA. Non-specific leakage of intracellular proteins was estimated by quantification of lactate dehydrogenase activity (U/L) in the cellular supernatants using a commercial assay. All results are given as means \pm S.D. and are normalized to the cell numbers (10^5 cells) releasing the indicated amount over 24 hrs.

(VEGF-R2/Flk-1) and vWF [34]. This was confirmed by RT-PCR in control cells after treatment with cAMP and retinoic acid (Fig. 3B, left part, compare [–] and [+] differentiation). Interestingly, in cells stably expressing GBP-1, the expression of both factors was increased to similar levels in the absence of cAMP and retinoic acid (Fig. 3B, right part, [–]) In line with this observation, expression levels of both factors were slightly up-regulated in GBP-1-transfected cells upon treatment with cAMP and retinoic acid (Fig. 3B, right part [+]). GBP-1 expression was not altered by treatment with cAMP and retinoic acid (Fig. 3B), and GAPDH levels demonstrated that equal amounts of RNA had been loaded (Fig. 3B). Quantitative evaluation of the results confirmed that induction by GBP-1 of both vWF and Flk-1 expression was similar

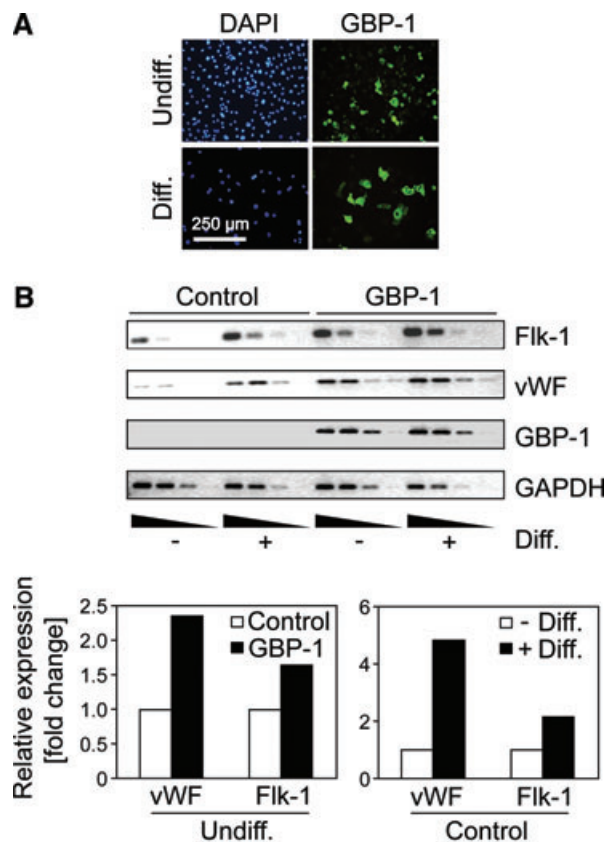


Fig. 3 After *in vitro* differentiation, GBP-1 expression is stably maintained and promotes EPC differentiation. **(A)** Staining of undifferentiated (Undiff.) and differentiated (Diff.) GBP-1-EPC by immunocytochemistry was performed with a rat anti-human GBP-1 antibody (green). Counterstaining was performed with DAPI (blue). **(B)** Semi-quantitative RT-PCR was performed to quantify RNA expression levels of Flk-1, vWF, GBP-1 and GAPDH in control- and GBP-1-EPC before (-) and after (+) differentiation. Decreasing amounts of cDNA (undiluted, 1:10, 1:100, 1:1000) were subjected to PCR after reverse transcription of the isolated RNA. Bands obtained at non-saturated levels were quantified by densitometry and normalized to the corresponding GAPDH signal. Results are given as fold change.

to that observed after standard treatment for differentiation (Fig. 3, lower-left panel, compare black [GBP-1] and white [control] bars; lower-right panel, white [undifferentiated], black [differentiated]). Overall, these results clearly indicate that GBP-1 expression was sufficient to induce the differentiation of EPC.

GBP-1 inhibits proliferation and migration of EPC *in vitro*

The proliferative and migratory behaviours of control- and GBP-1-EPC were investigated to evaluate whether GBP-1 expression impaired the EPC phenotype. Proliferation of GBP-1-EPC was

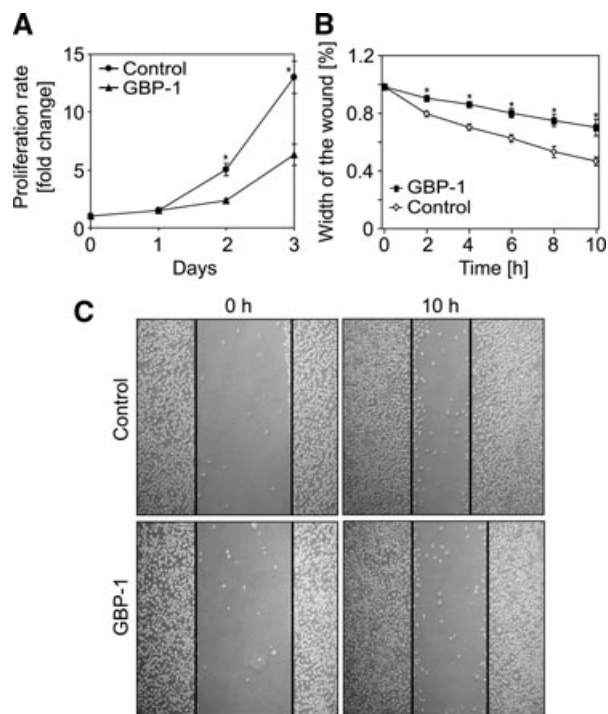


Fig. 4 GBP-1 reduces the proliferation and migration of EPC *in vitro*. **(A)** Control- and GBP-1-EPCs were cultured for 3 days after initial seeding of the same cell number and were counted every day with a Casy counter upon harvesting. Cell proliferation is expressed as fold induction. One representative experiment of at least three is shown, and data points are given as means \pm S.D. Asterisks indicate P -values ≤ 0.05 . **(B)** The migratory capacity of control- and GBP-1-EPC was investigated using a wound-healing assay. *In vitro* scratch wounds were generated by scraping a confluent cell monolayer with a sterile pipette tip. Pictures from the same areas were taken immediately after scratching (0 hr) and then every 2 hrs. The width of the scratch wounds at the time-points indicated was analysed and compared to the initial width. The values are displayed as relative percentages. Results are given as means \pm S.D. of one representative of at least four experiments. Asterisks indicate P -values ≤ 0.05 . **(C)** Representative pictures of the scratch assay acquired at time-points 0 and 10 hrs of Control- and GBP-1-EPC.

significantly ($P < 0.05$) inhibited compared to control-EPC (Fig. 4A). Moreover, time-course analysis employing the wound-healing assay showed that migration of GBP-1-EPC was significantly inhibited compared to control-EPC (Fig. 4B). The results obtained after 10 hr incubations clearly demonstrate the reduced capability of GBP-1-EPC to recultivate the wounded areas (Fig. 4C).

GBP-1 inhibits the migration of embryonic EPC *in vivo*

The migratory potential of the GBP-1-expressing and GBP-1-non-expressing T17b cells *in vivo* was studied in the AV-loop model of

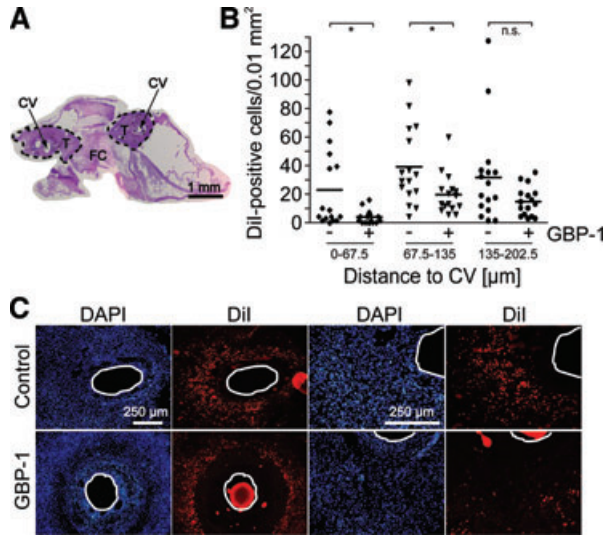


Fig. 5 Stable expression of GBP-1 reduces the migratory capacity of EPC in an *in vivo* AV-loop rat model. (A) Overview of an explant of the AV-loop chamber stained by haematoxylin/eosin. Letters indicate the anatomical structures central vessels (CV), fibrovascular tissue (T), and fibrin clot (FC), with the remaining being EPC. Scale bar = 1 mm. (B) The number of Dil⁺ cells/0.01 mm² tissue area was quantified in three relative distances to the CV at four different sites of each explant (*n* = 4 for each group). The values are depicted by a vertical scatter plot with a line corresponding to the mean. Asterisks are given for *P*-values ≤ 0.05; n.s. indicates not significant. (C) Dil⁺ Control- and GBP-1-EPC were visualized by epifluorescent microscopy (red). Counterstaining was performed with DAPI (blue). The lumen of the CV is indicated by a white line in the consecutive pictures. Different magnifications of the same areas are displayed (left versus right panel). The absolute numbers of cells in the DAPI channel were counted in at least three optical fields for both, the Control- and GBP-1-EPC, statistically evaluated and were not found to be significantly different (*P* = 0.474). Scale bars = 250 µm.

rats [40]. This method provides an *in vivo* compartment with defined size and similar initial vasculature as defined by the AV-loop, in contrast to other presently available *in vivo* tests, such as matrigel transplantation.

Equal amounts of Dil-labelled GBP-1- or control-EPC (5×10^6 cells) were inoculated as a fibrin suspension into AV-loop chambers (*n* = 8). After 14 days, the chambers were explanted and subjected to immunohistochemical analyses. Cross-sectioning and haematoxylin/eosin staining showed the central vessels (CV; Fig. 5A) of the AV-loop separated by the fibrin clot (FC) containing the EPC (Fig. 5A, FC). A fibrovascular tissue sheath (Fig. 5A, T) had developed, surrounding the CV.

EPC show directed migration to increasing oxygen gradients [41]. To determine the oxygen-directed migratory capacity of the implanted EPC, the numbers of Dil⁺ EPC were determined in defined squares (0.01 mm²) at three increasing distances (four squares at each distance) relative to the CV in representative tissue sections of each chamber (GBP-1-EPC, *n* = 4; control-EPC, *n* = 4). At the close distance (0–135 µm), the number of GBP-1-EPC was significantly reduced compared to the control-EPC (Fig. 5B). In

contrast, at the largest distance (>135 µm), cell densities of GBP-1-EPC and control-EPC were not statistically different (Fig. 5B). Representative histological pictures demonstrate this fact (Fig. 5C). GBP-1-EPC showed a clearly reduced capability to immigrate into the fibrovascular sheath towards increasing oxygen concentrations compared with control-EPC (Fig. 5C, compare GBP-1, Dil and control, Dil). The absolute numbers of cells present in the tissues did not differ in chambers filled with control-EPC or GBP-1-EPC, as indicated by DAPI staining (Fig. 5C, DAPI, *P* = 0.474).

Discussion

GBP-1 is the first GTPase shown to be secreted by cells [30]. Unfortunately, its extracellular function is still unclear. It has been shown that GBP-1 is selectively secreted by endothelial cells exposed to the inflammatory cytokines IFN-α/γ, IL-1α/β and TNF-α [30]. Increased serum concentrations of these cytokines are characteristically detected in patients with rheumatoid autoimmune disorders [16–18]. Consequently, activated endothelial cells have been detected in these patients at the tissue level, indicated by increased expression of the inflammation-associated proteins intercellular adhesion molecule 1 (ICAM-1) and vascular cell adhesion molecule 1 (VCAM) [42, 43]. Here, we show that GBP-1 serum levels may be used as a serologic marker for generalized inflammatory endothelial cell activation. Significantly increased serum levels of GBP-1 were detected by ELISA in patients with RA, SLE and SSc, as compared to healthy controls. The most robustly increased GBP-1 serum concentrations were observed in patients with RA (190.6 ± 301.6 ng/ml [RA] versus 17.5 ± 43.9 ng/ml [NHD]). In NHD and RA patients, 2.5% and 40% of the sera, respectively, contained more than 105.2 ng/ml GBP-1 (mean of NHD + 2 S.D.). These results identify GBP-1 as a novel biomarker for the detection of generalized inflammatory activation of endothelial cells in patients with rheumatic autoimmune disorders and favour the notion that IFN-inducible genes are involved in the etiopathogenesis of these diseases. Consistent with this notion, we recently reported that auto-antibodies against another IFN-inducible protein, the pro-inflammatory interferon, gamma-inducible protein 16 (IFI16), are significantly increased in patients with SSc, SLE and Sjogren syndrome [44, 45].

GBP-1 inhibits endothelial cell proliferation, migration and invasion [26–28], and inhibiting its expression abrogates these effects in endothelial cells exposed to inflammatory cytokines [16–18]. These findings established GBP-1 as the intracellular mediator of the anti-angiogenic effects on endothelial cells of inflammatory cytokines. Its anti-angiogenic activity has been confirmed in patients with colorectal carcinoma, where GBP-1 expression in tumour endothelial cells was associated with reduced angiogenic activity and significantly prolonged cancer-related survival of the patients [29]. Considering the anti-angiogenic effect of GBP-1 it is interesting that patients with rheumatic autoimmune diseases often present with cardiovascular dysfunction. This has mainly been attributed to the EPC system, which is often impaired

in these patients. The impact of GBP-1 on vasculogenic activities mediated by EPC has not been determined. In order to investigate this, we used a well-characterized EPC line, T17b, which can easily be transfected and differentiated by adding cAMP and retinoic acid *in vitro* [34]. The major cellular markers indicating EPC differentiation are Flk-1 and vWF. We found that both markers were strongly up-regulated in GBP-1-expressing EPC, indicating that GBP-1 is sufficient to induce premature differentiation of these cells. This finding is consistent with previous studies detecting circulating mature endothelial cells proposed to be released from vessel walls by shedding [5, 6].

GBP-1-induced EPC differentiation also impaired their vasculogenic activities by inhibition of their proliferation and migration *in vitro*. As yet, not many assays are available to quantify the migratory activities of cells *in vivo*. Matrigel-implant tests are often hampered by the fact that the pre-existing vasculature and volume spread of injected matrigel cannot be defined precisely [46]. To overcome these limitations, the rat AV loop model was established as a novel test system to investigate the migratory capability of EPC *in vivo*. In the AV loop model the vasculature is precisely defined by the vascular loop, and the reaction chamber permits the application of a defined amount of matrix in a defined structure with defined numbers of cells. As endothelial cells migrate along oxygen gradients *in vivo* [41], the migration of the applied EPC from the FC into the fibrovascular sheaths of the AV loop CV can be used to quantify cell migration. Employing this novel technology, we showed that control-EPC invaded the fibrovascular sheath significantly more efficiently than GBP-1-EPC cells. This confirmed that GBP-1 inhibits the migratory capability of EPC *in vivo*.

Taken together, our data establish circulating GBP-1 as a novel biomarker for inflammatory vessel activation in rheumatic autoimmune diseases. Mechanistically, GBP-1 induces the premature differentiation of EPC and inhibits the vasculogenic activities of EPC. Both effects most likely contribute to the cardiovascular defects observed as a major pathological impact in chronic autoimmune inflammatory diseases.

Acknowledgements

We thank Christina von Kleinsorgen, Melanie Nurtsch (all Division of Molecular and Experimental Surgery), Ilse Arnold, Katja Schubert and Stefan Fleischer (all Department of Plastic and Hand Surgery) for excellent technical assistance. This work was supported by grants of the Interdisciplinary Center for Clinical Research (IZKF) of the University Medical Center Erlangen to E.N./M.S. and M.H.; of the Deutsche Forschungsgemeinschaft to M.S. (DFG-SPP1130, DFG-GK1071, STU317/2-1), to MHe (SFB643-TPB5) and to U.K. (KN 578/2-1); of the ELAN program of the University Medical Center Erlangen to E.N. (AZ 08.10.30.1), to L.E.M. (AZ 09.03.18.1) and to O.B. (AZ 06.10.30.1); of the NIH to AKH (grant HL083958); of the Wucherpfennig-Stiftung to MHe; and of the Xue Hong and Hans Georg Geis Foundation to U.K. and R.H.

Conflict of interest

The authors confirm that there are no conflicts of interest.

References

- Carmeliet P. Mechanisms of angiogenesis and arteriogenesis. *Nat Med.* 2000; 6: 389–95.
- Carmeliet P. Angiogenesis in health and disease. *Nat Med.* 2003; 9: 653–60.
- Kilarski WW, Samolov B, Petersson L, *et al.* Biomechanical regulation of blood vessel growth during tissue vascularization. *Nat Med.* 2009; 15: 657–64.
- Risau W, Sariola H, Zerwes HG, *et al.* Vasculogenesis and angiogenesis in embryonic-stem-cell-derived embryoid bodies. *Development.* 1988; 102: 471–8.
- Ingram DA, Caplice NM, Yoder MC. Unresolved questions, changing definitions, and novel paradigms for defining endothelial progenitor cells. *Blood.* 2005; 106: 1525–31.
- Asahara T, Murohara T, Sullivan A, *et al.* Isolation of putative progenitor endothelial cells for angiogenesis. *Science.* 1997; 275: 964–7.
- Asahara T, Takahashi T, Masuda H, *et al.* VEGF contributes to postnatal neovascularization by mobilizing bone marrow-derived endothelial progenitor cells. *EMBO J.* 1999; 18: 3964–72.
- Takahashi T, Kalka C, Masuda H, *et al.* Ischemia- and cytokine-induced mobilization of bone marrow-derived endothelial progenitor cells for neovascularization. *Nat Med.* 1999; 5: 434–8.
- Shaked Y, Ciarrocchi A, Franco M, *et al.* Therapy-induced acute recruitment of circulating endothelial progenitor cells to tumors. *Science.* 2006; 313: 1785–7.
- Rafii S, Lyden D, Benezra R, *et al.* Vascular and haematopoietic stem cells: novel targets for anti-angiogenesis therapy? *Nat Rev Cancer.* 2002; 2: 826–35.
- Kuwana M, Kaburaki J, Okazaki Y, *et al.* Increase in circulating endothelial precursors by atorvastatin in patients with systemic sclerosis. *Arthritis Rheum.* 2006; 54: 1946–51.
- Westerweel PE, Luijten RK, Hoefer IE, *et al.* Haematopoietic and endothelial progenitor cells are deficient in quiescent systemic lupus erythematosus. *Ann Rheum Dis.* 2007; 66: 865–70.
- Herbrig K, Haensel S, Oelschlaegel U, *et al.* Endothelial dysfunction in patients with rheumatoid arthritis is associated with a reduced number and impaired function of endothelial progenitor cells. *Ann Rheum Dis.* 2006; 65: 157–63.
- Grisar J, Aletaha D, Steiner CW, *et al.* Depletion of endothelial progenitor cells in the peripheral blood of patients with rheumatoid arthritis. *Circulation.* 2005; 111: 204–11.
- Avouac J, Uzan G, Kahan A, *et al.* Endothelial progenitor cells and rheumatic disorders. *Joint Bone Spine.* 2008; 75: 131–7.

16. **Banchereau J, Pascual V.** Type I interferon in systemic lupus erythematosus and other autoimmune diseases. *Immunity.* 2006; 25: 383–92.
17. **Karonitsch T, Feierl E, Steiner CW, et al.** Activation of the interferon-gamma signaling pathway in systemic lupus erythematosus peripheral blood mononuclear cells. *Arthritis Rheum.* 2009; 60: 1463–71.
18. **Brennan FM, McInnes IB.** Evidence that cytokines play a role in rheumatoid arthritis. *J Clin Invest.* 2008; 118: 3537–45.
19. **Ablin JN, Boguslavski V, Aloush V, et al.** Effect of anti-TNF α treatment on circulating endothelial progenitor cells (EPCs) in rheumatoid arthritis. *Life Sci.* 2006; 79: 2364–9.
20. **Prakash B, Praefcke GJ, Renault L, et al.** Structure of human guanylate-binding protein 1 representing a unique class of GTP-binding proteins. *Nature.* 2000; 403: 567–71.
21. **Prakash B, Renault L, Praefcke GJ, et al.** Triphosphate structure of guanylate-binding protein 1 and implications for nucleotide binding and GTPase mechanism. *EMBO J.* 2000; 19: 4555–64.
22. **Schwemmler M, Staeheli P.** The interferon-induced 67-kDa guanylate-binding protein (hGBP1) is a GTPase that converts GTP to GMP. *J Biol Chem.* 1994; 269: 11299–305.
23. **Naschberger E, Bauer M, Stürzl M.** Human guanylate binding protein-1 (hGBP-1) characterizes and establishes a non-angiogenic endothelial cell activation phenotype in inflammatory diseases. *Adv Enzyme Regul.* 2005; 45: 215–27.
24. **Tripal P, Bauer M, Naschberger E, et al.** Unique features of different members of the human guanylate-binding protein family. *J Interferon Cytokine Res.* 2007; 27: 44–52.
25. **Lubeseder-Martellato C, Guenzi E, Jörg A, et al.** Guanylate-binding protein-1 expression is selectively induced by inflammatory cytokines and is an activation marker of endothelial cells during inflammatory diseases. *Am J Pathol.* 2002; 161: 1749–59.
26. **Guenzi E, Töpolt K, Cornali E, et al.** The helical domain of GBP-1 mediates the inhibition of endothelial cell proliferation by inflammatory cytokines. *EMBO J.* 2001; 20: 5568–77.
27. **Guenzi E, Töpolt K, Lubeseder-Martellato C, et al.** The guanylate binding protein-1 GTPase controls the invasive and angiogenic capability of endothelial cells through inhibition of MMP-1 expression. *EMBO J.* 2003; 22: 3772–82.
28. **Weinländer K, Naschberger E, Lehmann MH, et al.** Guanylate binding protein-1 inhibits spreading and migration of endothelial cells through induction of integrin α 4 expression. *FASEB J.* 2008; 22: 4168–78.
29. **Naschberger E, Croner RS, Merkel S, et al.** Angiostatic immune reaction in colorectal carcinoma: impact on survival and perspectives for antiangiogenic therapy. *Int J Cancer.* 2008; 123: 2120–9.
30. **Naschberger E, Lubeseder-Martellato C, Meyer N, et al.** Human guanylate binding protein-1 is a secreted GTPase present in increased concentrations in the cerebrospinal fluid of patients with bacterial meningitis. *Am J Pathol.* 2006; 169: 1088–99.
31. **Hochberg MC.** Updating the American College of Rheumatology revised criteria for the classification of systemic lupus erythematosus. *Arthritis Rheum.* 1997; 40: 1725.
32. **Arnett FC, Edworthy SM, Bloch DA, et al.** The American Rheumatism Association 1987 revised criteria for the classification of rheumatoid arthritis. *Arthritis Rheum.* 1988; 31: 315–24.
33. **LeRoy EC, Black C, Fleischmajer R, et al.** Scleroderma (systemic sclerosis): classification, subsets and pathogenesis. *J Rheumatol.* 1988; 15: 202–5.
34. **Hatzopoulos AK, Folkman J, Vasile E, et al.** Isolation and characterization of endothelial progenitor cells from mouse embryos. *Development.* 1998; 125: 1457–68.
35. **Bleiziffer O, Horch RE, Hammon M, et al.** T17b murine embryonal endothelial progenitor cells can be induced towards both proliferation and differentiation in a fibrin matrix. *J Cell Mol Med.* 2009; 13: 926–35.
36. **Vajkoczy P, Blum S, Lamparter M, et al.** Multistep nature of microvascular recruitment of ex vivo-expanded embryonic endothelial progenitor cells during tumor angiogenesis. *J Exp Med.* 2003; 197: 1755–65.
37. **Schellerer VS, Croner RS, Weinländer K, et al.** Endothelial cells of human colorectal cancer and healthy colon reveal phenotypic differences in culture. *Lab Invest.* 2007; 87: 1159–70.
38. **Arkudas A, Tjiawi J, Saumweber A, et al.** Evaluation of blood vessel ingrowth in fibrin gel subject to type and concentration of growth factors. *J Cell Mol Med.* 2009; 13: 2864–74.
39. **Polykandriotis E, Euler S, Arkudas A, et al.** Regression and persistence: remodelling in a tissue engineered axial vascular assembly. *J Cell Mol Med.* 2009. DOI: 10.1111/j.1582-4934.2009.00828.x
40. **Arkudas A, Tjiawi J, Bleiziffer O, et al.** Fibrin gel-immobilized VEGF and bFGF efficiently stimulate angiogenesis in the AV loop model. *Mol Med.* 2007; 13: 480–7.
41. **Decaris ML, Lee CI, Yoder MC, et al.** Influence of the oxygen microenvironment on the proangiogenic potential of human endothelial colony forming cells. *Angiogenesis.* 2009; 12: 303–11.
42. **Belmont HM, Buyon J, Giorno R, et al.** Up-regulation of endothelial cell adhesion molecules characterizes disease activity in systemic lupus erythematosus. The Schwartzman phenomenon revisited. *Arthritis Rheum.* 1994; 37: 376–83.
43. **Yusuf-Makagiansar H, Anderson ME, Yakovleva TV, et al.** Inhibition of LFA-1/ICAM-1 and VLA-4/VCAM-1 as a therapeutic approach to inflammation and autoimmune diseases. *Med Res Rev.* 2002; 22: 146–67.
44. **Mondini M, Vidali M, De Andrea M, et al.** A novel autoantigen to differentiate limited cutaneous systemic sclerosis from diffuse cutaneous systemic sclerosis: the interferon-inducible gene IFI16. *Arthritis Rheum.* 2006; 54: 3939–44.
45. **Caposio P, Gugliesi F, Zannetti C, et al.** A novel role of the interferon-inducible protein IFI16 as inducer of proinflammatory molecules in endothelial cells. *J Biol Chem.* 2007; 282: 33515–29.
46. **Cornali E, Zietz C, Benelli R, et al.** Vascular endothelial growth factor regulates angiogenesis and vascular permeability in Kaposi's sarcoma. *Am J Pathol.* 1996; 149: 1851–69.